Inorg. Chem. **2003**, *42*, 4018–4028

Two-Electron-Transfer Redox Systems, Part 7:† Two-Step Electrochemical Oxidation of the Boron Subhalide Cluster Dianions $B_6X_6^{2-}$ (X = Cl, Br, I)

Bernd Speiser,* Tina Wizemann, and Marc WUrde

Institut für Organische Chemie, Auf der Morgenstelle 18, D-72076 Tübingen, Germany

Received January 30, 2003

Boron subhalide cluster dianions $B_6X_6^{2-}$ (X = Cl, Br, I) are electrochemically oxidized in two steps. According to cyclic voltammograms, the first step is chemically reversible and yields the corresponding radical anions $B_6X_6^{\bullet-}$. The electron transfer is nearly diffusion controlled. The second, slower electron-transfer step leads to a species which we assume to be the hitherto not yet described neutral compounds $B_6X_6^0$. The voltammograms indicate a coupled fast catalytic reaction, producing the radical anions in a reduction by an electrolyte component. Computer simulations of the cyclic voltammograms reveal mechanistic details of the redox reactions, as well as quantitative values for formal potentials, rate constants, and diffusion coefficients. The results are compared to other B_nX_n redox systems.

Introduction

According to WADE's rules,[2] boranes with $(2n + 2)$ binding electrons form *closo*-cages. The stable dianions of boron subhalides, $B_nX_n^{2-}$ (X = hal, n = 6, 8−12), are among the most prominent examples.[3] Many of their structures have been characterized and are based on *n*-vertex deltahedra (n = 6: ref 4, n = 9: ref 5, n = 10: ref 6, n = 11: ref 7). Clusters with only $2n$ binding electrons are often also stable and possess similar structures. Although they are exceptions to Wade's rules, such hypercloso compounds have been isolated in the boron subhalide series, e.g., for X = Cl and n = 8 and 9.[8,9] Their stability is explained by a combination of the π-donor properties of the halogen atoms and steric effects.[10] Similar stabilization was observed for $B_{12}(OCH_2Ph)_{12}$.[11]

Various reports of electrochemical redox transformations between *closo*-dianionic and *hypercloso*-neutral boron subhalide clusters with n = 8−11 consistently show that the two electrons are transferred in separate one-electron steps at distinguishable redox (or formal) potentials E^0.[6,7,9,12,13] The E^0 of the two steps are separated by several hundred mV, a result which is also found for the benzyloxy−B_{12} cluster mentioned above.[11] This "normal" potential ordering is usually an indication that no appreciable reorganization of the molecular structure is involved in the redox reactions.[14] Changes in bond lengths and angles between the clusters $B_9Br_9^{0/\bullet-/2-}$ have been investigated in detail.[5]

The question is still open if this behavior is also followed by cages with less than eight boron atoms. One could easily imagine that clusters with a smaller number of boron atoms

* To whom correspondence should be adressed. E-mail: bernd.speiser@uni-tuebingen.de. Phone: +49 (7071) 29-76205. Fax: +49 (7071) 29-5518.

† Part 6, see ref 1.

(1) Ludwig, K.; Quintanilla, M. G.; Speiser, B.; Stauss, A. *J. Electroanal. Chem.* **2002**, *531*, 9−18.
(2) Wade, K. *Adv. Inorg. Chem. Radiochem.* **1976**, *18*, 1−66.
(3) Morrison, J. A. The Polyhedral Boron Monohalides: Prototypical Electron-Deficient Cluster Compounds. In *Advances in Boron and the Boranes*; Liebman, J. F., Greenberg, A., Williams, R. E., Loker, D. P., Loker, K. B., Eds.; VCH: Weinheim, Germany, 1988; Vol. 5.
(4) Preetz, W.; Peters, G. *Eur. J. Inorg. Chem.* **1999**, 1831−1846.
(5) Hönle, W.; Grin, Y.; Burkhardt, A.; Wedig, U.; Schultheiss, M.; von Schnering, H. G.; Kellner, R.; Binder, H. *J. Solid State Chem.* **1997**, *133*, 59−67.
(6) Einholz, W.; Vaas, K.; Wieloch, C.; Speiser, B.; Wizemann, T.; Ströbele, M.; Meyer, H.-J. *Z. Anorg. Allg. Chem.* **2002**, *628*, 258−268.
(7) Volkov, O.; Paetzold, P.; Hu, C.; Kölle, U. *Z. Anorg. Allg. Chem.* **2001**, *627*, 1029−1033.
(8) Morrison, J. A. *Chem. Rev.* **1991**, *91*, 35−48.
(9) Speiser, B.; Tittel, C.; Einholz, W.; Schäfer, R. *J. Chem. Soc., Dalton Trans.* **1999**, 1741−1751.
(10) McKee, M. L.; Wang, Z.-X.; von Ragué Schleyer, P. *J. Am. Chem. Soc.* **2000**, *122*, 4781−4793.
(11) Peymann, T.; Knobler, C. B.; Khan, S. I.; Hawthorne, M. F. *Angew. Chem.* **2001**, *113*, 1713−1715.
(12) Bowden, W. *J. Electrochem. Soc.* **1982**, *129*, 1249−1252.
(13) Binder, H.; Kellner, R.; Vaas, K.; Hein, M.; Baumann, F.; Wanner, M.; Winter, R.; Kaim, W.; Hönle, W.; Grin, Y.; Wedig, U.; Schultheiss, M.; Kremer, R. K.; von Schnering, H. G.; Groeger, O.; Engelhardt, G. *Z. Anorg. Allg. Chem.* **1999**, *625*, 1059−1072.
(14) Evans, D. H.; Hu, K. *J. Chem. Soc., Faraday Trans.* **1996**, *92*, 3983−3990.

10.1021/ic034101k CCC: $25.00
Published on Web 05/28/2003

are subject to increasingly serious structural changes as a response to the addition or removal of electrons. This might result in "potential inversion",[14] a situation which is characterized by the instability of the intermediate (radical anion) oxidation state with respect to disproportionation.[9,14] In particular, electrochemical techniques such as cyclic voltammetry can be used to detect such behavior.

The next smaller well-known and structurally characterized analogues are the 6-vertex boron subhalide dianions ($B_6X_6^{2-}$, X = Cl, Br, I; derivatives with various combinations of halogen atoms).[4,15−19] Their boron atoms form a close to octahedral core.[20]

Up to now, only the one-electron oxidation of the $B_6X_6^{2-}$ to radical anions $B_6X_6^{\bullet-}$ has been investigated by chemical and electrochemical means,[4] and redox potentials were qualitatively correlated with the steric and electronic effects of the halogen atoms in the cluster.[19] Detailed analyses of IR/Raman[18,21] and ESR spectra[17,18] as well as X-ray crystal structure determinations[19] and quantum mechanical calculations[22] of the oxidized species revealed exceptional stabilities of the monoanions, but no dramatic structural rearrangement if compared to the dianionic parent compounds.

No evidence for further oxidation to neutral clusters has been described as yet. We report here for the first time the occurrence of a second oxidation in the B_6X_6 series (X = Cl, Br, I) which leads to (under the solution conditions used) unstable two-electron oxidation products of the dianionic starting compounds. This seems to be the first evidence for the existence of neutral $B_6X_6^0$.

Experimental Section

Starting Compounds. The tetra-*n*-propylammonium salts of the clusters $B_6X_6^{2-}$ (X = Cl, Br, I)[16] were received from Prof. Dr. W. Preetz, Institut für Anorganische Chemie, Christian-Albrechts-Universität, Kiel, Germany, and were used without further purification.

Electrochemical Experiments. Dichloromethane (Burdick and Jackson, stabilized with cyclohexene) was distilled through a packed column and then dried over activated Al_2O_3 (basic, activated at 400 °C and 10^{-4} mbar for 4 h). Tetra-*n*-butylammonium hexafluorophosphate, NBu_4PF_6, was prepared from NBu_4Br and NH_4PF_6 or recycled as described before.[23] It was used in a concentration of 0.1 M in the base electrolyte.

The electrolyte was degassed by three freeze−pump−thaw cycles before it was transferred into the electrochemical cell under argon.

All electrochemical experiments were performed with a Bioanalytical Systems (BAS, West Lafayette, IN) 100 B/W electrochemical workstation controlled via a standard personal computer (control program version 2.0). For electroanalytical experiments, a Pt electrode tip of Metrohm (Filderstadt, Germany) was used as the working electrode. The electroactive area ($A = 0.071$ cm^2) of the Pt disk was determined from cyclic voltammograms, and chronoamperograms as well as chronocoulograms of ferrocene (fc).[24] The counter electrode was a coiled Pt wire of 1-mm diameter. A single-unit Haber-Luggin double-reference electrode[25] was used in most experiments. The resulting potential values refer to Ag/Ag^+ (0.01 M in CH_3CN/0.1 M NBu_4PF_6). Fc was used as an external standard. Its potential was determined by separate cyclic voltammetric experiments, and all potentials were then rescaled to E^0 (fc/fc$^+$) = +0.211 V vs Ag/Ag^+. All potentials in the present paper are given relative to the fc standard.[26]

For cyclic voltammetry, a gastight full-glass three-electrode cell, whose assembly for the experiments was described previously, was used.[23] The cell was purged with argon prior to filling it with electrolyte. Background curves were recorded before adding substrate to the solution. These were later subtracted from the experimental data with substrate. The automatic BAS 100 B/W *iR*-drop compensation facility was used for all experiments.

For preparative bulk electrolyses, working and counter electrodes were nets of Pt/Ir, 90/10 (Degussa, Hanau, Germany). They were separated from each other by a glass frit. The reference electrode was similar to the one described above. This cell was also gastight and could be thermostated. It was purged with argon prior to filling it with electrolyte.

Numerical simulations[27] were performed with the commercial DigiSim software (BAS; version 2.1; FIFD algorithm, default numerical options).[28] Semi-infinite planar diffusion was assumed. The preequilibrium option of the program was enabled for chemical equilibria only. The temperature was set to 298.2 K, and all transfer coefficients of the electron transfers were assumed to be 0.5, while both the uncompensated resistance and the double layer capacitance were set to zero in the simulations.

ESR Spectroscopy. The ESR spectra were recorded with a Bruker ESP 300 spectrometer.

Results and Discussion

General Voltammetric Behavior. The tetra-*n*-propylammonium salts of the cluster dianions $B_6Cl_6^{2-}$, $B_6Br_6^{2-}$, and $B_6I_6^{2-}$ are easily soluble in CH_2Cl_2 and were electrochemically investigated in a CH_2Cl_2/0.1 M NBu_4PF_6 electrolyte. The open circuit potentials of the dianion solutions are $E_{oc} \approx -0.310$ V ($B_6Cl_6^{2-}$), −0.170 V ($B_6Br_6^{2-}$), and −0.135 V ($B_6I_6^{2-}$). Cyclic voltammograms of the $B_6Cl_6^{2-}$ and $B_6Br_6^{2-}$ dianions with starting potentials close to the corresponding E_{oc} exhibited three well-separated oxidation signals in the accessible potential range of the electrolyte (peaks I, III, and

(15) Fritze, J.; Preetz, W.; Marsmann, H. C. *Z. Naturforsch. B: Chem. Sci.* **1987**, *42*, 287−292.
(16) Preetz, W.; Fritze, J. *Z. Naturforsch. B: Chem. Sci.* **1984**, *39*, 1472−1477.
(17) Lorenzen, V.; Preetz, W.; Baumann, F.; Kaim, W. *Inorg. Chem.* **1998**, *37*, 4011−4014.
(18) Wanner, M.; Kaim, W.; Lorenzen, V.; Preetz, W. *Z. Naturforsch., B: Chem. Sci.* **1999**, *54*, 1103−1108.
(19) Heinrich, A.; Keller, H.-L.; Preetz, W. *Z. Naturforsch. B: Chem. Sci.* **1990**, *45*, 184−190.
(20) Thesing, J.; Baurmeister, J.; Preetz, W.; Thiery, D.; von Schnering, H. G. *Z. Naturforsch. B: Chem. Sci.* **1991**, *46*, 800−808.
(21) Lorenzen, V.; Preetz, W. *Z. Naturforsch. B: Chem. Sci.* **1997**, *52*, 565−572.
(22) Burkhardt, A.; Wedig, U.; von Schnering, H. G.; Savin, A. *Z. Anorg. Allg. Chem.* **1993**, *619*, 437−441.
(23) Dümmling, S.; Eichhorn, E.; Schneider, S.; Speiser, B.; Würde, M. *Curr. Sep.* **1996**, *15*, 53−56.
(24) Speiser, B.; Würde, M.; Maichle-Mössmer, C. *Chem.−Eur. J.* **1998**, *4*, 222−233.
(25) Gollas, B.; Krauss, B.; Speiser, B.; Stahl, H. *Curr. Sep.* **1994**, *13*, 42−44.
(26) Gritzner, G.; Kůta, J. *Pure Appl. Chem.* **1984**, *56*, 461−466.
(27) Speiser, B. Numerical Simulation of Electroanalytical Experiments: Recent Advances in Methodology. In *Electroanalytical Chemistry*; Bard, A. J., Rubinstein, I., Eds.; Marcel Dekker: New York, 1996; Vol. 19.
(28) Rudolph, M.; Reddy, D. P.; Feldberg, S. W. *Anal. Chem.* **1994**, *66*, 589A−600A.

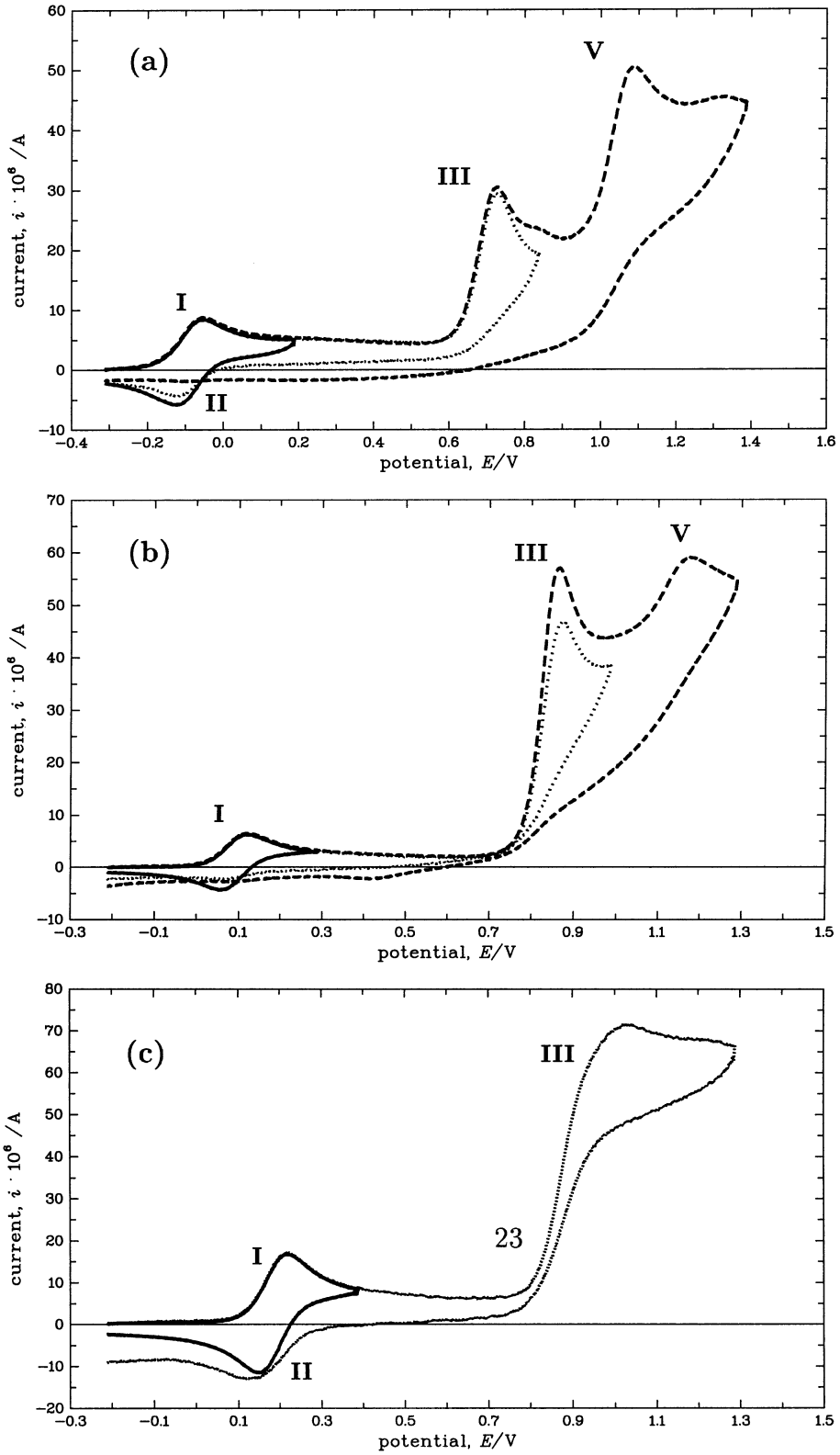

Figure 1. Cyclic voltammograms of $B_6X_6^{2-}$ in CH_2Cl_2/0.1 M NBu_4PF_6 at a Pt disk electrode: (a) X = Cl, (b) X = Br, (c) X = I; ν = 1.0 V s^{-1}, c = 0.217 mM (a); 0.125 mM (b); 0.316 mM (c); solid lines: potential range of first oxidation; dotted lines: switching potential selected to include the second oxidation peak; broken lines: switching potential selected to include the third oxidation signal.

V; parts a and b of Figure 1), whereas only two signals were observed in the case of $B_6I_6^{2-}$ (Figure 1c). For X = Cl and I, at potentials immediately after the second (and, for X = Cl, also the third) peak, additional weak oxidation waves appear, depending on the time scale of the experiments. In the case of the chloro cluster, these signals are more developed at higher concentrations. They might thus be related to products of second- or higher-order follow-up reactions. The cyclic voltammograms of $B_6Br_6^{2-}$ do not exhibit such signals. No reduction of any of the dianions is

Table 1. Parameters Characterizing the Redox Process $B_6X_6^{2-} \rightleftharpoons B_6X_6^{\bullet -}$ in CH_2Cl_2/0.1 M NBu_4PF_6

X	E^0/V	k_{s1}[c]	D[d]
Cl	−0.088[a]		$4.0 \pm 0.4 \times 10^{-6}$ [a]
	−0.097[b]	64[e]	4.58×10^{-6} [b]
Br	+0.089[a]		$6.7 \pm 0.2 \times 10^{-6}$ [a]
	+0.090[b]	0.25	5.96×10^{-6} [b]
I	+0.180[a]		$7.3 \pm 0.5 \times 10^{-6}$ [a]
	+0.185[b]	0.0977	7.58×10^{-6} [b]

[a] From quantitative analysis of the cyclic voltammograms; mean values from various independent experiments; E^0 from midpoint potentials. [b] From simulations of cyclic voltammograms with DigiSim and fitting to the experimental current/potential curves. [c] Heterogeneous rate constant of oxidation to radical anions, in cm s^{-1}. [d] In cm^2 s^{-1}. [e] Nominal value from fitting procedure, not significant due to diffusion control.

obvious in the accessible potential range investigated (to ~ -1.2 V).

From the results of these overall cyclic voltammograms, more quantitative experiments were planned: for various concentrations c^0 were recorded cyclic voltammograms and chronocoulograms, extending over (a) the first oxidation only and (b) the first *and* the second electron-transfer processes. The third oxidation and the weak signals were not investigated in detail. However, exhaustive controlled potential electrolyses were performed at the potential of the primary oxidation step with the additional goal to identify the formation of radical anions by ESR spectroscopy.

Cyclic Voltammetry of First Oxidation Step. Selected and typical cyclic voltammograms of $B_6Cl_6^{2-}$, $B_6Br_6^{2-}$, and $B_6I_6^{2-}$ in the potential range of the first oxidation signal are presented in Figure 1 (solid lines) and exhibit peaks I (oxidation) and II (rereduction). Their qualitative appearance is in accordance with earlier results by other authors.[17,19] The peak potential difference ΔE_p is only slightly increasing with the potential scan rate υ and approaches the theoretical value (0.058 V) for a diffusion-controlled (electrochemically reversible) one-electron process at small υ. The peak potentials and the midpoint potentials, $\bar{E}$, are almost independent of υ. Consequently, the $\bar{E}$ are a good estimate for the formal redox potential E^0 of the first oxidation step of eq 1

$$B_6X_6^{2-} \rightleftharpoons B_6X_6^{\bullet -} + e^- \qquad (1)$$

of the $B_6X_6^{2-}$ to the corresponding $B_6X_6^{\bullet -}$ radical anions (Table 1). All potential values are essentially independent of c^0, indicating nearly complete compensation of the *iR* drop in the electrolyte. Only for the highest scan rates used does a slight increase of ΔE_p with increasing c^0 become apparent.

In accordance with the potential data, the peak current function $i_p^I/\sqrt{\upsilon}c^0$ for X = Cl, Br is independent of υ and c^0. From i_p^I it is possible to estimate the diffusion coefficient D according to ref 29 (Table 1). In the case of X = I, a slight decrease of $i_p^I/\sqrt{\upsilon}c^0$ with increasing υ is observed. This may be caused by a transition to quasi-reversibility at high υ for this compound. Still, estimation of D is possible for $B_6I_6^{2-}$ because the variation of $i_p^I/\sqrt{\upsilon}c^0$ is weak. The peak current ratio i_p^{II}/i_p^I (calculated according to Nicholson's equation[30]) is close to unity and, in particular, independent of υ. This indicates chemical reversibility of the redox process and thus the persistency of the $B_6X_6^{\bullet -}$ on the time scale of these experiments.

Electrolytic Oxidation of $B_6X_6^{2-}$ (X = Cl, Br). The chloro and bromo clusters in the investigated series of compounds were anodically oxidized in bulk electrolysis experiments. In both cases, a potential was applied that was more positive than E^0, but not high enough to reach the onset of the second oxidation wave. The current through the cell was integrated, resulting in a value for the total charge transferred. From this charge and the amount of starting compound, the number of electrons transferred was calculated as $n = 0.81$ ($B_6Cl_6^{2-}$) and $n = 1.0$ ($B_6Br_6^{2-}$), confirming that the first oxidation signal corresponds to a one-electron transfer in both cases. In accordance with earlier reports,[4] the solution turned yellow-green ($B_6Cl_6^{2-}$) or yellow-orange ($B_6Br_6^{2-}$). These colors correspond to those of the radical anions.[4]

When the solution of $B_6Cl_6^{\bullet -}$ was transferred into an ESR tube and frozen, a broad ESR signal with a *g*-factor of 2.014 was recorded. The latter value is close to the corresponding results reported earlier for $B_6Cl_6^{\bullet -}$ (2.027)[17] and for other $B_nCl_n^{\bullet -}$ ($n = 8$: 2.017,[9] $n = 9$: 2.018,[9] $n = 10$: 2.029[6]). The spectrum did not show any hyperfine structure. In the case of $B_6Br_6^{\bullet -}$, no ESR spectrum could be detected after transfer to the spectrometer at either 293 or 77 K, although this radical anion was characterized earlier after chemical oxidation in the frozen state.[17]

Simulation of Cyclic Voltammograms for First Oxidation Step. Cyclic voltammograms of all three cluster dianions in the potential region of the first oxidation step were simulated with DigiSim[28] under the assumption of a quasi-reversible one-electron redox process according to eq 1. In all three cases, very good agreement between experimental and simulated curves could be established using a single set of system parameters (E^0; heterogeneous rate constant of electron transfer, k_{s1}; transfer coefficient, $\alpha_1 = 0.5$) for the voltammograms of a particular cluster at all υ and c^0 (Table 1; see Supporting Information for selected voltammograms of $B_6I_6^{2-}$). Hence, the mechanistic hypothesis describes the oxidation process well.

The formal potentials from the fitting procedure agree well (Table 1) with those determined directly from the current/potential curves. They increase with the size of the halogen substituent, as observed before.[4,19] The absolute values cannot easily be compared to those reported in the literature, but the extent of the substituent effect agrees within 10 mV (see also below discussion of substituent and cluster size effects). The increase of E^0 with the size of the halogen substituent was explained by the decreasing ability to back-donate electrons from the halogen π-orbitals to the boron atoms in the cage.[19]

(29) Nicholson, R. S.; Shain, I. *Anal. Chem.* **1964**, *36*, 706−723.

(30) Nicholson, R. S. *Anal. Chem.* **1966**, *38*, 1406.

The diffusion coefficients from the optimized simulations compare well with those directly calculated from the peak current data above (Table 1).

In addition to the parameters already determined from the voltammograms directly, the simulations also yield values for k_{s1}. These rate constants (Table 1) decrease with increasing size of the halogen, i.e., the activation barrier for the one-electron oxidation becomes increasingly higher if we go from X = Cl to Br and I, possibly because of increasing steric strain. Although the results from the fitting procedure show that $B_6Cl_6^{2-}$ is oxidized in a diffusion-controlled process, $B_6Br_6^{2-}$ and $B_6I_6^{2-}$ show already mixed diffusion/electron-transfer kinetics control. The value of k_{s1} for $B_6Cl_6^{2-}$ is only a nominal value resulting from the fitting procedure: At the scan rates used in the present work, the electron-transfer kinetics for the one-electron oxidation of the chloro-dianion is too fast[31] to estimate a significant value for this reaction parameter. In the case of the iodo compound, on the other hand, the simulation results confirm the conclusion of quasi-reversibility.

Cyclic Voltammetry Including the Second Oxidation Step. Cyclic voltammograms in a potential region extending after the second oxidation signal (peak III, Figures 1−4) of the cluster dianions reveal a much more complex behavior than those discussed for the first step. For X = Cl and Br, no reverse peak related to peak III is present, not even at high scan rates ($v \leq 50$ V s^{-1}). Thus, the second oxidation step of these clusters is chemically irreversible at all time scales used. Only for X = I at $v \geq 20$ V s^{-1} does a reverse peak IV begin to appear (see Figure 5 for $v = 50$ V s^{-1}). Recently, we had observed a reverse peak for the second oxidation step starting from $B_{10}X_{10}^{2-}$ (X = Cl, Br) at fast voltammetric time scales, indicating that the $B_{10}X_{10}^{0}$ have short but finite lifetimes under these conditions.[6] In comparison, we interpret the product of the second oxidation of $B_6I_6^{2-}$ as $B_6I_6^{0}$. The B_6I_6 cluster seems to have a persistency comparable to $B_{10}X_{10}^{0}$. On the other hand, $B_9X_9^{0}$ and $B_8X_8^{0}$ quickly react in the CH_2Cl_2 electrolyte used in the present work.[9] In comparison, the stability of hypothetically neutral $B_6X_6^{0}$ clusters (X = Cl, Br), if formed in peak III, is lower than that of $B_6I_6^{0}$.

The peak potentials E_p^{III} (Table 2), dependent on v, shift to more positive values with increasing scan rates by up to several 10 mV per decade of v. Because a simple first-order reaction of the $B_6X_6^{0}$ would result in a shift of only ~30 mV per decade, quasi-reversibility contributes to this strong shift. Furthermore, in the intermediate v range around 2 V s^{-1}, peak III becomes superimposed with the additional weak signal. In some voltammograms, peak III is severely distorted and a peak potential cannot be determined. The concentration dependence of the peak potentials is small at slow time scales. Some stronger dependence occurs only at the highest scan rates.

The peak current function $i_p^{III}/\sqrt{v}c^0$ is much larger than $i_p^{I}/\sqrt{v}c^0$ (see Table 3 for the peak current ratio i_p^{III}/i_p^{I}). The value of i_p^{III} was determined from a baseline extrapolated from the decreasing part of peak I (BAS 100 B/W control program). For simple stepwise two-electron systems, i_p^{III}/i_p^{I} should approach a value of unity. This limit is almost reached for $B_6I_6^{2-}$ and high scan rates, which indicates that the second oxidation step is indeed also a one-electron process. The most likely product is then $B_6X_6^{0}$.

For X = Br and Cl and for smaller v even in the case of X = I, however, i_p^{III}/i_p^{I} is much larger than unity and further increases with decreasing scan rate. In the case of the chloro and the iodo clusters, the concentration dependence of i_p^{III}/i_p^{I} is weak. For $B_6Br_6^{2-}$, however, a considerable increase is observed for decreasing concentration, and at $c^0 = 0.047$ mM, extremely high values of i_p^{III}/i_p^{I} are reached.

These peak current data indicate that an increased flux of electroactive material to the electrode is present in the second as compared to the first oxidation step. Such behavior is explained by the mechanism which was originally observed for $B_nCl_n^{0}$ ($n = 8, 9$)[9] and later for $n = 10$ systems (X = Cl, Br).[6] In comparison, we assume that the neutral clusters $B_6X_6^{0}$ formed at the electrode are reduced in the electrolyte (homogeneous electron transfer) to yield $B_6X_6^{\bullet -}$. At the potentials of peak III, the radical anion can of course be reoxidized to $B_6X_6^{0}$ (heterogeneous electron transfer at the electrode surface). Consequently, we describe the overall redox reaction in peak III by reactions 2 and 3

$$B_6X_6^{\bullet -} \overset{-e^-}{\rightleftharpoons} B_6X_6^{0} \text{ (heterogeneous)} \qquad (2)$$

$$B_6X_6^{0} + e^- \rightarrow B_6X_6^{\bullet -} \text{ (homogeneous)} \qquad (3)$$

Spectroscopic results[9] have shown that traces of residual water in the solvent are responsible for this reduction, possibly through partial hydrolysis of B−B bonds in some of the starting compound.

Chronocoulometry. The Anson plots[32] of chronocoulometric data for the first oxidation steps of the $B_6X_6^{2-}$ (X = Cl, Br) are linear and do not show an intercept. We conclude that adsorption of the clusters, both in the dianionic and the monoanionic form, is negligible. The ratio $Q(2\tau)/Q(\tau)$ is close to the value 0.414 expected for a chemically reversible oxidation process. In accordance with the cyclic voltammetric results discussed above, $Q(2\tau)/Q(\tau)$ approaches unity if the potential step is extended over the second oxidation process. This confirms the fast chemical reaction of the $B_6X_6^{0}$. Also, in accordance with the "catalytic reaction" hypothesis, the Anson plot slope is much more than twice the value if one steps across the second oxidation signal as compared to an experiment only involving the primary one-electron oxidation. For the simple stepwise two-electron system, we would expect an increase by a factor of 2.

Simulation of Cyclic Voltammograms including the First and Second Oxidation Steps. To confirm the validity of the mechanistic hypothesis (eq 2)/(eq 3) for the second oxidation and to estimate thermodynamic and kinetic parameters for the various reaction steps, the cyclic voltam-

(31) Matsuda, H.; Ayabe, Y. *Z. Elektrochem.* **1955**, *59*, 494−503.

(32) Kim, J.; Faulkner, L. R. *Anal. Chem.* **1984**, *56*, 874−880.

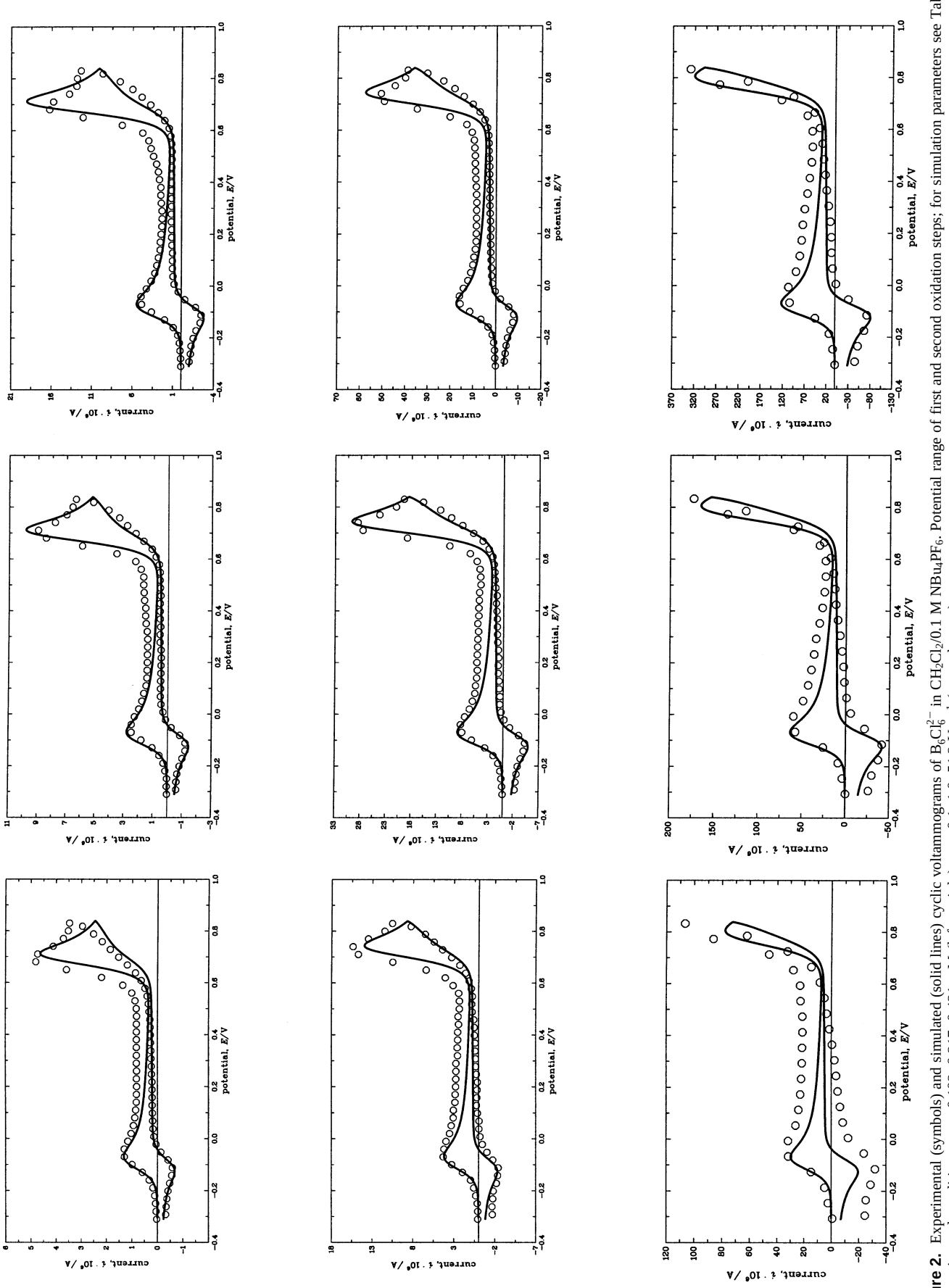

Figure 2. Experimental (symbols) and simulated (solid lines) cyclic voltammograms of $B_6Cl_6^{2-}$ in CH_2Cl_2/0.1 M NBu_4PF_6. Potential range of first and second oxidation steps; for simulation parameters see Table 4; experimental conditions: $c = 0.102$, 0.217, 0.421 mM (left to right), $\nu = 0.1$, 1.0, 51.2 V s^{-1} (top to bottom).

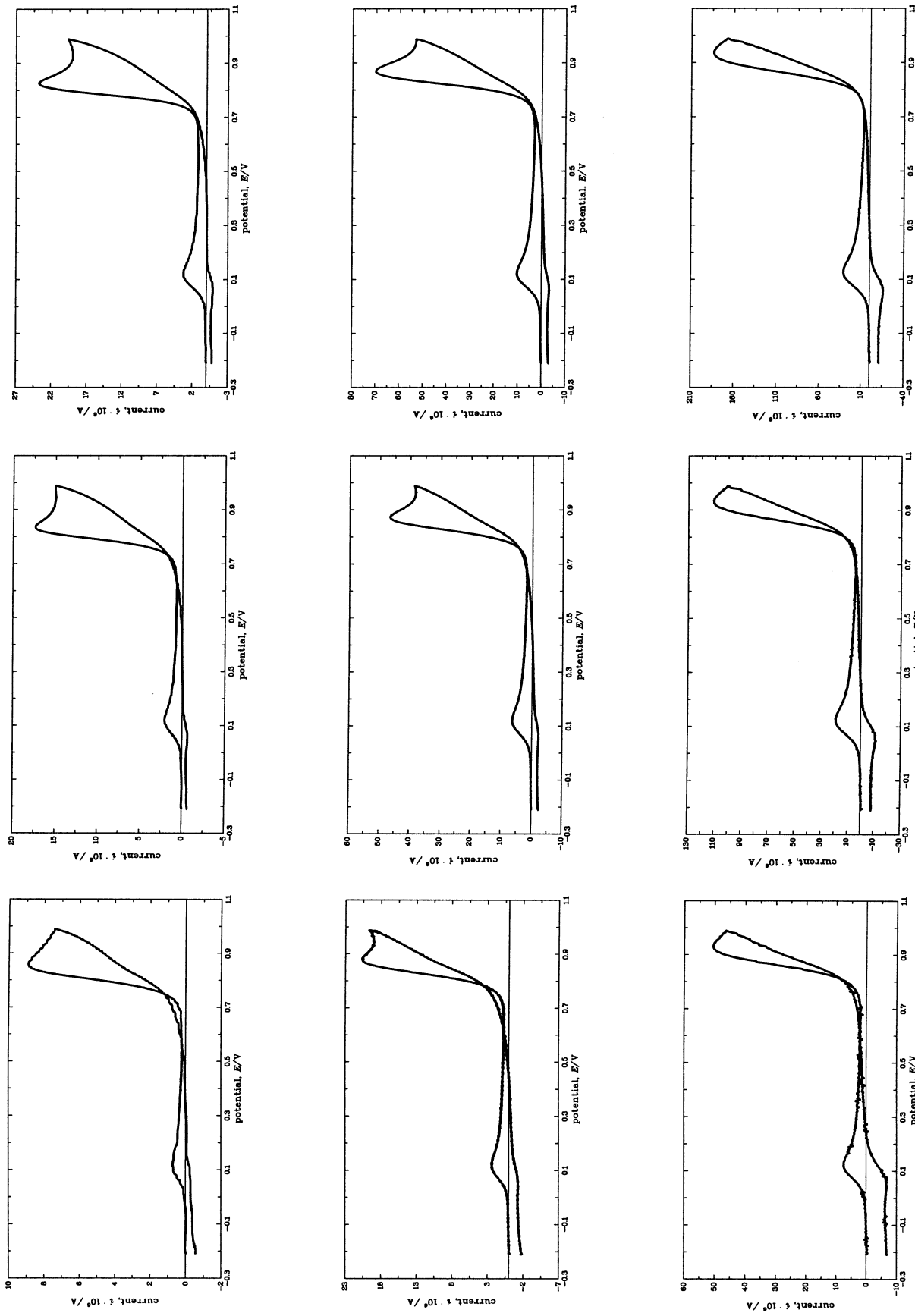

Figure 3. Experimental cyclic voltammograms of $B_6Br_6^{2-}$ in CH_2Cl_2/0.1 M NBu_4PF_6. Potential range of first and second oxidation steps; experimental conditions: c = 0.047, 0.125, 0.197 mM (left to right), ν = 0.1, 1.0, 10.24 V s^{-1} (top to bottom).

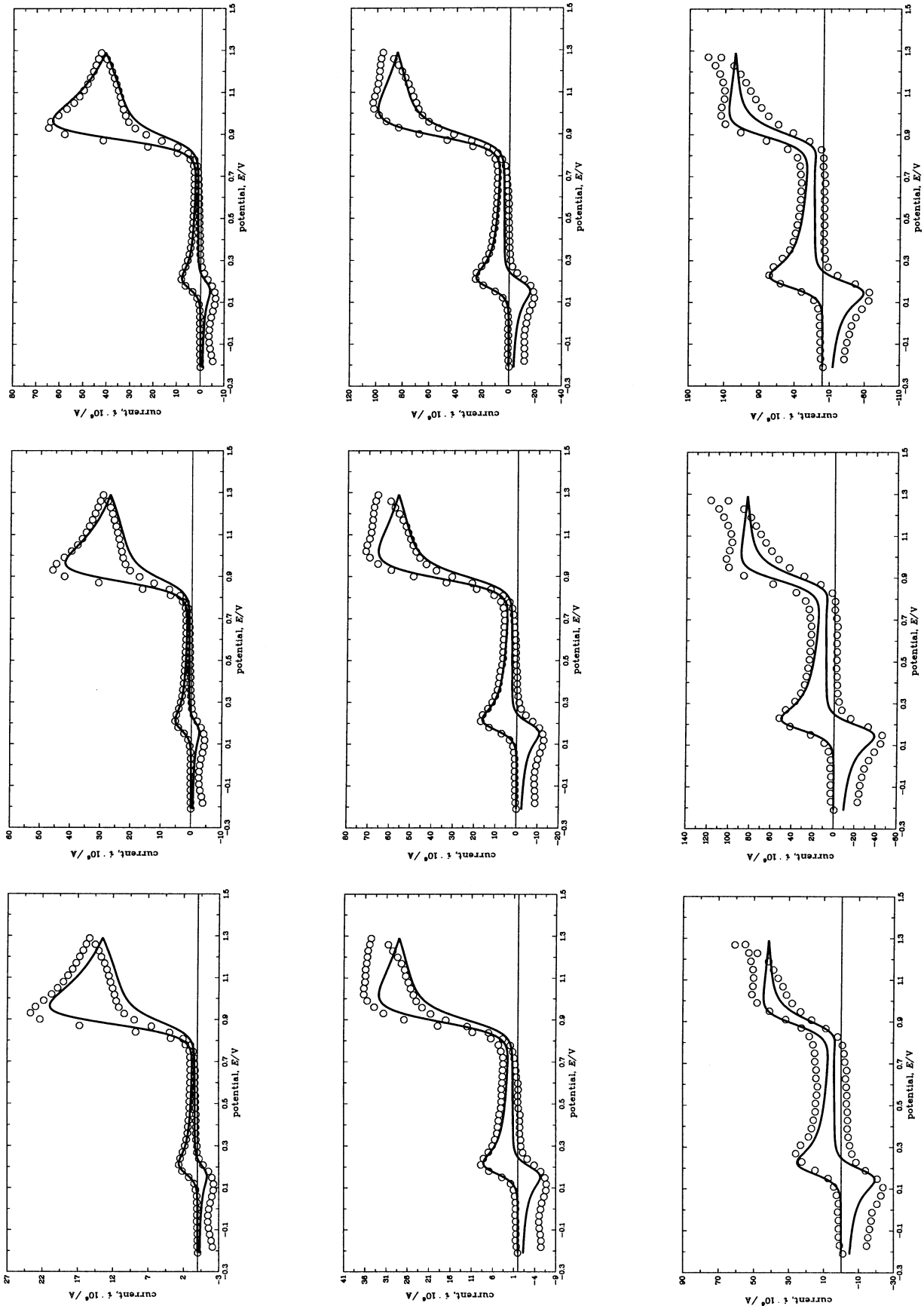

Figure 4. Experimental (symbols) and simulated (solid lines) cyclic voltammograms of $B_6I_6^{2-}$ in CH_2Cl_2/0.1 M NBu_4PF_6. Potential range of first and second oxidation steps; for simulation parameters see Table 4; experimental conditions: $c = 0.158$, 0.316, 0.477 mM (left to right), $\upsilon = 0.1$, 1.0, 10.24 V s^{-1} (top to bottom).

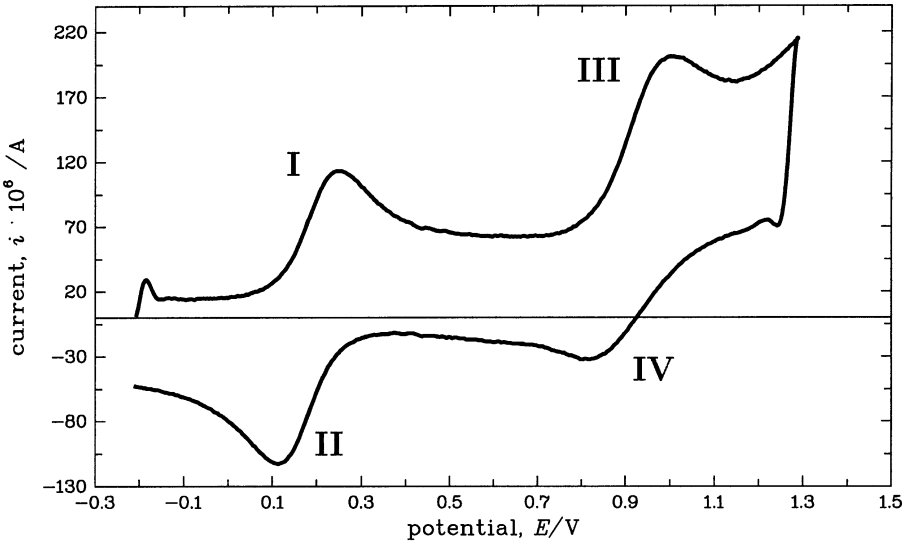

Figure 5. Cyclic voltammogram of $B_6I_6^{2-}$ in CH_2Cl_2/0.1 M NBu_4PF_6; $c = 0.316$ mM, $\upsilon = 50$ V s^{-1}.

Table 2. Peak Potentials E_p^{II} for the Second Oxidation Peak in Cyclic Voltammograms of $B_6X_6^{2-}$

	$B_6Cl_6^{2-}$			$B_6Br_6^{2-}$			$B_6I_6^{2-}$		
υ/Vs^{-1}	0.102 mM	0.217 mM	0.421 mM	0.047 mM	0.125 mM	0.197 mM	0.158 mM	0.316 mM	0.477 mM
0.02	+0.660	+0.669	+0.669	+0.767	+0.806	+0.801	+1.113	+1.116	+1.118
0.05	+0.687	+0.683	+0.681	+0.840	+0.847	+0.814	+1.129	+1.132	+1.137
0.1	+0.695	+0.696	+0.692	+0.853	+0.827	+0.824	+1.143	+1.144	+1.151
0.2	+0.702	+0.701	+0.703	+0.858	+0.839	+0.837	+1.152	+1.158	+1.225
0.5	+0.724	+0.717	+0.720	+0.867	+0.858	+0.857	+1.189	+1.191	+1.205
1.0	+0.729	+0.729	+0.752	+0.876	+0.870	+0.896	+1.260	+1.241	+1.258
2.0	+0.745	+0.743	+0.745	+0.891	+0.887	+0.886	+1.444	[a]	+1.370
5.12	+0.767	+0.800	+0.775	+0.912	+1.005	+0.916	+1.174	+1.198	+1.209
10.24	+0.783	+0.784	+0.797	+0.930	+0.935	+0.938	+1.245	+1.184	+1.207
20.48	+0.898	+0.815	+0.850	+1.002	+0.960	+0.972	+1.172	+1.192	+1.205
51.2	+0.825	+0.867	+0.909	+1.014	+1.015	+1.029	+1.174	+1.212	+1.238

[a] Peak overlapping with a further, weak signal at slightly higher potential.

Table 3. i_p^{III}/i_p^{I} in Cyclic Voltammograms of $B_6X_6^{2-}$ Clusters

	$B_6Cl_6^{2-}$			$B_6Br_6^{2-}$			$B_6I_6^{2-}$		
υ/Vs^{-1}	0.102 mM	0.217 mM	0.421 mM	0.047 mM	0.125 mM	0.197 mM	0.158 mM	0.316 mM	0.477 mM
0.02	3.83	3.17	2.56	22.85	9.27	7.94	12.37	11.84	10.79
0.05	3.67	3.11	2.60	12.56	9.06	7.19	10.01	9.74	9.35
0.1	3.42	2.91	2.55	10.67	8.57	7.34	8.84	8.50	7.89
0.2	3.46	3.05	2.68	10.71	8.17	7.15	7.30	7.08	6.54
0.5	3.52	3.41	2.87	10.19	7.80	6.86	5.39	5.27	4.96
1.0	3.61	3.44	2.68	9.49	8.11	6.26	3.89	4.01	3.72
2.0	3.64	3.51	3.00	8.83	7.81	6.61	3.47	3.39	3.18
5.12	3.49	2.95	3.04	8.27	6.53	6.24	2.01	2.05	1.89
10.24	3.48	3.66	2.94	6.96	6.21	5.81	1.59	1.73	1.62
20.48	2.29	3.88	3.64	5.94	5.81	5.56	1.51	1.55	1.47
51.2	2.84	3.06	2.91	5.03	5.08	4.85	1.34	1.47	1.36

mograms of the $B_6X_6^{2-}$ in the potential range extending over the first *and* second oxidation waves were simulated and the results fitted to the experimental curves. Voltammograms for $0.02 \le \upsilon \le 51.2$ V s^{-1} and all c^0 were used for the fitting process. Only voltammograms for X = Cl and I could successfully be simulated (Figures 2 and 4). To generate satisfactory agreement between experiment and simulation for all compounds, an additional reaction step

$$B_6X_6^0 \rightarrow P \qquad (4)$$

had to be included, in which the neutral cluster reacted to an as yet unidentified product P. We assume this reaction to be essentially irreversible. In the context of the DigiSim simulation program, however, reaction 4 had to be formulated as an equilibrium step with a large equilibrium constant K_4 (K_4 was set to a fixed value of 10^{10}; changes of K_4 from this value did not influence the simulation results to an appreciable extent).

The parameter values determined above from voltammograms in the potential range of the first wave (Table 1) were used for these more complex calculations, and the corresponding parameters were not subject to variation in the fitting procedure. The most important parameters varied were the formal potential E^0 ($B_6X_6^{\bullet -}/B_6X_6^0$), the heterogeneous

Table 4. Simulation Parameters for the Cyclic Voltammograms of Two-Step Oxidation of $B_6X_6^{2-}$

	X =	
params	Cl	I
E^0 ($B_6X_6^{2-}/B_6X_6^{\bullet-}$)/V[a]	−0.097	+0.185
k_{s1}/cm s^{-1} [a]	64	0.0977
α_1[b]	0.5	0.5
E^0 ($B_6X_6^{\bullet-}/B_6X_6^{0}$)/V[c]	+0.775	+0.882
k_{s2}/cm s^{-1} [c]	0.5245	0.0413
α_2[b]	0.5	0.5
K_3[d]	2.259×10^{18}	2.966×10^{18}
k_3/s^{-1} [c]	2×10^4	1.8×10^2
K_4[b,e]	10^{10}	10^{10}
k_4/s^{-1} [c]	9.557×10^3	11.01
D/cm^2 s^{-1} [a]	4.58×10^{-6}	7.58×10^{-6}

[a] From simulations of cyclic voltammograms of first oxidation step; see Table 1. [b] Fixed value. [c] Determined by fitting of simulations to experimental cyclic voltammograms. [d] Value determined by DigiSim during detection of "thermodynamically superfluous reactions". [e] Large value selected in order to model irreversible chemical reaction.

rate constant for the second electron transfer k_{s2}, and the rate constants k_3 and k_4 of reactions 3 and 4, respectively, which were assumed to be of (pseudo) first order. In comparison to α_1 in the simulations discussed before, the transfer coefficient α_2 was fixed at a value of 0.5. Again, reaction 3 is necessarily an equilibrium reaction in the DigiSim formulation. However, the value of the corresponding equilibrium constant K_3 is determined by the two formal redox potentials as a so-called "thermodynamic superfluous reaction" parameter.[33]

Results from the fitting procedure for X = Cl and I are given in Table 4. Qualitatively, simulated voltammograms based on reactions 1−4 give reasonable to excellent agreement to the experimental current/potential curves over the entire range of v and c^0 investigated. In particular, the height, shape, and position of peak III as well as the height of peak II can be reproduced. In the case of X = I, the transition from an S-shaped wave III at high scan rates (Figure 4, bottom) to a peak-shaped signal at lower scan rates (Figure 4, top) indicates the presence of reaction 4 consuming $B_6I_6^0$. If $B_6I_6^0$ were only undergoing reduction to the radical anion in reaction 3, a current plateau would be expected even at small values of v. In fact, the features of peak III are extremely sensitive to the values of the rate constants k_3 and k_4, as well as their ratio.

In the B_6Cl_6 redox series, the S-shaped form of the voltammograms is never reached in accordance with a considerably increased rate constant k_4 for the decay of the neutral cluster $B_6Cl_6^0$, as compared to the rate for the decay of $B_6I_6^0$. The combined action of reactions 3 and 4 determines the persistency of the neutral clusters, and the slower rates in the iodo case are consistent with the observation of reduction peak IV at fast time scales (Figure 5).

A further interesting phenomenon appears from these calculations: the heterogeneous electron-transfer rate constants k_{s2} are smaller than those for the first electron transfer. This may indicate some influence of geometric changes, making the transfer of the second electron slow. A similar effect had been observed for the B_nCl_n (n = 8, 9) series.[9]

The analysis in the section "Cyclic Voltammetry Including the Second Oxidation Step" has already shown that $B_6Br_6^{2-}$ might present a more complex behavior than $B_6Cl_6^{2-}$ and $B_6I_6^{2-}$. Indeed, simulation of the $B_6Br_6^{2-}$ voltammograms proved unsuccessful with the mechanistic scheme discussed. Although qualitatively similar (occurrence of peak III with high intensity, missing reduction peak IV), some second- or higher-order reactions must be involved to account for the concentration dependence of i_p^{III}/i_p^{I}. Peak II is much smaller as compared to the voltammograms of the other two clusters. Furthermore, the bromo cluster voltammograms (Figure 3) exhibit the striking feature of "curve crossing"[34−41] at low scan rates and concentrations.

Curve (or trace) crossing usually requires the presence of two redox steps linked by a chemical reaction (ECE mechanism) and the so-called "cross reaction", which interconverts the redox partners of these two processes.[34,35] Hence, we tested mechanistic hypotheses that involved an ECE process in peak III starting from $B_6Br_6^{\bullet-}$. However, all attempts to model the behavior of peak III with these mechanisms failed. Also, the decreased intensity of peak II could only be simulated with additional decay reactions. Consequently, no simulations for the $B_6Br_6^{2-}$ voltammograms are shown, and we do not present quantitative results for the second oxidation of $B_6Br_6^{\bullet-}$ to $B_6Br_6^0$.

Effects of Halide Substituents and Cluster Size. Boron subhalide clusters with a variety of cluster sizes and halide atom substituents have been investigated in recent years with regard to their redox properties, in particular the redox potentials in the three-species redox series $B_nX_n^{0/\bullet-/2-}$ (Table 5). In all cases, well-separated two-step redox reactions from neutral via radical anionic to dianionic clusters are observed. The difference of the formal potentials ΔE^0 for the $B_nX_n^{0/\bullet-}$ and the $B_nX_n^{\bullet-/2-}$ redox processes is usually several 100 mV, with no particular tendency toward either cluster size or substituent. In none of the cases is potential compression[42] or inversion[14] apparent. Only a decrease of k_{s2} is obvious. Although for the oxidation of $B_6H_6^{2-}$ geometrical distortion is expected from quantum mechanical considerations,[10,43] such behavior is not indicated in the B_6X_6 series by any unusual ΔE^0. A possible explanation may be the commonly accepted π-back-donation of electron density

(33) Luo, W.; Feldberg, S. W.; Rudolph, M. *J. Electroanal. Chem.* **1994**, *368*, 109−113.
(34) Feldberg, S. W. *J. Phys. Chem.* **1971**, *75*, 2377−2380.
(35) Amatore, C.; Pinson, J.; Savéant, J. M.; Thiebault, A. *J. Electroanal. Chem.* **1980**, *107*, 59−74.
(36) Andrieux, C. P.; Merz, A.; Savéant, J. M. *J. Am. Chem. Soc.* **1985**, *107*, 6097−6103.
(37) Fox, M. A.; Akaba, R. *J. Am. Chem. Soc.* **1983**, *105*, 3460−3463.
(38) Gaudiello, J. G.; Wright, T. C.; Jones, R. A.; Bard, A. J. *J. Am. Chem. Soc.* **1985**, *107*, 888−897.
(39) Dietrich, M.; Heinze, J.; Fischer, H.; Neugebauer, F. A. *Angew. Chem.* **1986**, *98*, 999−1000.
(40) Hinkelmann, K.; Mahlendorf, F.; Heinze, J.; Schacht, H.-T.; Field, J. S.; Vahrenkamp, H. *Angew. Chem.* **1987**, *99*, 373−374.
(41) Dietrich, M.; Heinze, J.; Krieger, C.; Neugebauer, F. A. *J. Am. Chem. Soc.* **1996**, *118*, 5020−5030.
(42) Evans, D. H. *Acta Chem. Scand.* **1998**, *52*, 194−197.
(43) O'Neill, M. E.; Wade, K. *Inorg. Chem.* **1982**, *21*, 461−464.

Table 5. Formal or (if mentioned) Peak Potentials of Redox Processes in the $B_nX_n^{0/\bullet-/2-}$ Series [$E_1^0 = E^0(B_nX_n^{\bullet-}/B_nX_n^{2-})$, $E_2^0 = E^0(B_nX_n^0/B_nX_n^{\bullet-})$][k]

	X = Cl		Br		I	
n	E_1^0	E_2^0	E_1^0	E_2^0	E_1^0	E_2^0
6[a]	−0.097	+0.775	+0.090	[b]	+0.185	+0.882
6[c]	(+0.577)		(+0.769)		(+0.884)	
8[d]	+0.067	+0.959				
9[d]	+0.112	+0.600				
9[e]	(−0.63)	(−0.10)	(−0.72)	(−0.24)	(−0.74)	(−0.33)
10[f]	+1.01	+1.73	+1.14	+1.77		
11[g]	+1.1[h]	[i]	+0.97	>+1.3[h]	+1.3[h]	+1.5[h]
12[j]	+1.92					

[a] This work. [b] Not available (see discussion of simulations). [c] Vs Ag/AgCl/LiCl in ethanol from ref 17. [d] From ref 9. [e] From ref 13, reported vs a glassy-carbon pseudo-reference electrode. [f] From ref 6. [g] From ref 7. [h] Not reversible; peak or approximate values. [i] Badly separated from first peak. [j] From ref 12, differential pulse voltammetric peak; reported vs Ag/AgCl, recalculated vs fc/fc^+ by comparing the E^0 values of $B_{10}X_{10}^{2-}$ in ref 6 and 12; no second oxidation observed. [k] Values in parentheses cannot be recalculated to the fc/fc^+ reference scale.

from the halide atoms to the boron cage, which might attenuate the effect of the two-electron loss.

A comparison of individual potentials for either of the two redox processes is hampered by the use of different reference electrodes by various groups and the possible occurrence of diffusion potentials. While in the present work, as well as in references 6 and 9, potentials are referred to the fc/fc^+ standard reference redox system recommended by IUPAC,[26] other authors present data vs a saturated calomel electrode,[7] which can be recalculated vs fc/fc^+ with the information provided. Some results for the $B_6X_6^{\bullet-/2-}$ [17] and the $B_9X_9^{0/\bullet-/2-}$ [13] series are reported vs a halide-susceptible-reference electrode or a pseudo-reference electrode without giving a value of E^0 (fc/fc^+). In these cases recalculation is impossible, and absolute values cannot be compared to the fc/fc^+-referenced data. Furthermore, in the $B_{11}X_{11}$ series, irreversible waves occur.[7] In contrast to the E^0 of reversible processes, their peak potentials are not only determined by the thermodynamics but also by the kinetics of the redox process. Consequently, these values are also not quantitatively comparable to E^0 data. The single potential value for $B_{12}X_{12}^{2-}$ was determined by differential pulse polarography.[12] Despite the fact that this value is reported vs a Ag/AgCl reference electrode, recalculation can be attempted by comparing the values for $B_{10}X_{10}^{2-}$ in the same paper and our results.[9]

A tendency for an increase of E^0 with the size of the halide substituent can be observed for the B_6X_6 and the $B_{10}X_{10}$ clusters, whereas the opposite effect is apparent for the data of the B_9X_9, and in the $B_{11}X_{11}$ compounds no clear pattern is found. If we only compare fc/fc^+-referenced potentials, on the other hand, there is a strong increase of the redox potentials with *n* for the first oxidation process starting from the $B_nX_n^{2-}$. Interestingly, there seems to be a large break between the $n = 9$ and the $n = 10$ compounds, with E^0 ($B_nX_n^{\bullet-}/B_nX_n^{2-}$) of the clusters with $n \geq 10$ being shifted to rather high positive potentials. Hence, these compounds are much more difficult to oxidize than expected. The reason for such a gap is not clear at present.

Conclusion

The data of this work clearly show that the boron subhalide cluster dianions $B_6X_6^{2-}$ (X = Cl, Br, I) are oxidized in two separate steps through radical anions to neutral compounds which then undergo a fast rereduction with a solvent component. The stability of the neutral $B_6X_6^0$ is sufficient to detect this species at fast voltammetric scan rates. Thus, despite their smaller size, the B_6X_6 clusters behave analogously to the clusters with $n = 8-11$ boron atoms. The results presented here extend the knowledge of the redox chemistry in the series of the B_nX_n to smaller cages. Also, they indicate that $B_6X_6^0$ species exist and could possibly be isolated under carefully controlled conditions.

However, several questions remain. In particular, it seems important to study the redox properties of the smallest boron subhalide clusters, $B_4X_4^{0/\bullet-/2-}$, of which $B_4Cl_4^0$ is known,[5,22,44] although its stability is low. Furthermore, the nature of the reaction products indicated by the weak peaks in the cyclic voltammograms of the $B_6X_6^{2-}$ and the reason why the bromo cluster's kinetic behavior deviates from that of the other compounds investigated here may be worth pursuing in further work.

Acknowledgment. We thank the Fonds der Chemischen Industrie, Frankfurt/Main, Germany, for financial assistance to T.W. We gratefully acknowledge samples of the boron cluster dianion salts, which were supplied by Prof. Dr. W. Preetz, Institut für Anorganische Chemie, Christian-Albrechts-Universität, Kiel, Germany. We also thank Andreas Stauss for performing preliminary experiments with the chloro and bromo clusters and Paul Schuler for the ESR experiments.

Supporting Information Available: Experimental and simulated cyclic voltammograms of $B_6I_6^{2-}$ in CH_2Cl_2/0.1 M NBu_4PF_6, first oxidation step. This material is available free of charge via the Internet at http://pubs.acs.org.

IC034101K

(44) Atoji, M.; Lipscomb, W. N. *Acta Crystallogr.* **1953**, *6*, 547−550.